TECHNICAL MEMORANDUMS

NATIONAL ADVISORY COMMITTEE FOR AERONAUTICS

No. 428

DRAG MEASUREMENTS ON A JUNKERS WING SECTION

Application of the Betz Method to the Results of Comparative Tests Made on a Model and on an Airplane in Flight

By Hanns Weidinger

From "Berichte und Abhandlungen der Wissenschaftlichen Gesellschaft für Luftfahrt, December, 1926

Washington
September, 1927

NATIONAL ADVISORY COMMITTEE FOR AERONAUTICS.

TECHNICAL MEMORANDUM NO. 428.

DRAG MEASUREMENTS ON A JUNKERS WING SECTION.*

Application of the Betz Method to the Results of Comparative Tests Made on a Model and on an Airplane in Flight.

By Hanns Weidinger.

Introduction

The design of an airplane must be based on exhaustive theoretical calculations and practical tests conducted both with models and with airplanes in flight. Particular and thorough knowledge of the resultant air force which acts upon the wing is required. It produces drag, pressure, deflection, and torsional stresses. So far, no exhaustive investigations on this air force are available. This refers particularly to drag. There are two drag components: the "induced" drag and the "profile" or wing-section drag. While the induced drag, which is simply due to losses at the wing tips, is theoretically measurable with a fair degree of accuracy, no method has been yet developed for directly calculating or measuring the profile drag, which depends on the shape of the wing section. In "Zeitschrift für Flugtechnik und Motorluftschiffahrt," of February 14, 1925 (see N.A.C.A. Technical Memorandum No. 337), A. Betz published

*"Profilwiderstands-Messungen an einem Tragflügel." From "Berichte und Abhandlungen der Wissenschaftlichen Gesellschaft für Luftfahrt," December, 1926.

the theoretical bases of a method for the direct determination of the profile drag. Betz suggested that this method be applied to wind-tunnel tests as well as to full-scale measurements. Thus an adequate solution of the question of drag distribution over the entire span is obtained.

The comparison of model tests with tests in flight can be based on the result of such measurements. They are very important from the aerodynamical point of view, as they lead to useful conclusions regarding the behavior of the wing, its best shape and the conformity of theoretical and actual flow. Although there still remains a certain prejudice against such measurements, I have attempted to make these comparative tests in order to inspire confidence in the reliability and demonstrate the importance of measurements in flight.

I. Betz Method for the Direct Determination of Wing-Section Drag*

The profile or wing-section drag is ordinarily found by measuring the total wing drag in a wind tunnel. The profile drag is then obtained by subtracting the calculated induced drag from the total drag. The trouble with this method is that the profile drag is obtained from the difference of two values of the same magnitude. Hence, if the total and the induced drag cannot be determined with absolute accuracy, the resulting error

*From "Zeitschrift für Flugtechnik und Motorluftschiffahrt," 1925, No. 3, p. 42 ff.

will be comparatively great, owing to the smallness of the profile drag. The total drag is usually measured on a considerably reduced model with a small index value. The calculation of the induced drag is only approximately correct and the disregarded points affect the profile drag. Thus this method appears to be only a makeshift giving a rather low degree of accuracy.

J. Ackeret, in his newly developed method, calculates the profile drag directly from the energy loss of the air, thereby proceeding from the tests dealing with velocity and pressure distribution behind airfoils, which were published in the second volume of the "Ergebnisse der Aerodynamischen Versuchsanstalt zu Gottingen."

In connection with the rules for efficiency tests* of fans and compressors, the following symbols were adopted.

p_{st} Static pressure: the internal pressure of a gas flowing in a straight line, hence the pressure which would be indicated by an instrument moving with the gas at the same velocity.

q Dynamic (or impact) pressure: the highest increase of pressure developed in a gas stream in front of an obstacle. It is equal to the pressure required to accelerate the gas at rest to the given velocity. The formula of the impact pressure is

$$q = \frac{\rho}{2} v^2 \text{ kg/m}^2$$

*"Zeitschrift des Vereines deutscher Ingenieure," 1925.

where $\rho = \frac{\gamma}{g}$ denotes the density of the gas expressed in $\frac{kg/s^2}{m^4}$.

v = the mean velocity of flow expressed in m/s.

p_g Total pressure: the algebraic sum of the static and the impact pressures.

According to Bernoulli's law, the sum of static and dynamic pressures is constant in a steady flow without losses (potential flow). It is

$$p_{st} + q = p_g = \text{constant}.$$

If losses occur during the course of the flow, the total pressure behind the obstacle cannot be as high as in front of it. Thus, from the difference of the total pressures in a plane behind and in front of the wing, the energy loss of the flow at this wing section can be directly measured in this plane. By means of the energy loss, we are enabled to determine the wing-section drag, as will be shown farther along.

The advantage derived from this method is the easy determination of the profile drag for any wing section from which the distribution of the profile drag over the span can be easily deduced. This is an important point, as most of the new wing types are neither rectangular nor characterized by a constant thickness, but are usually tapered toward the tips. Another advantage results from the fact that this method is not confined to model tests, but can be applied to measurements in flight, as

will be shown in the main part of this treatise. This fact is of fundamental importance, as it has now become fully apparent that the data required for new designs are better determined in flight than in the laboratory or on the test bench.

Point 1.- In order to simplify the calculation of the profile-drag formula, Betz first considered a body which developed no lift but only drag. Moreover, two-dimensional flow was assumed. In front of the body the static pressure is p_{st_o} and the velocity v_o. The total pressure in the undisturbed flow is then

$$p_{g_o} = p_{st_o} + \frac{\rho}{2} v_o^2 = p_{st_o} + q_o = \text{constant}$$

Likewise, behind the body

$$p_{g_1} = p_{st_1} + \frac{\rho}{2} v_1^2 = \text{constant} = p_{g_o},$$

where p_{st_1} is the static pressure and v_1 the velocity behind the body. Only in a small vortical portion directly behind the body

$$p_{g_1} < p_{g_o}.$$

The drag is determined by means of the momentum formula. A control surface is considered to be behind and in front of the body. This surface is assumed to be infinite upward and downward, but equal in its other dimension to the span l. The flow exerts a certain force on the body, which produces variations in the pressure and momentum. The pressure on the surface $l\ dy$ in front of the wing is

$$p_{st_o}\ l\ dy \left[\frac{kg}{m^2}\ m\ m = kg\right].$$

The pressure on the plane $l\,dy$ behind the wing is

$$p_{st_1}\, l\, dy\ [kg].$$

The pressure variation with reference to the two infinite surfaces is then

$$l \int_{-\infty}^{+\infty} (p_{st_o} - p_{st_1})\, dy.$$

According to the momentum law, the impulse of the force in any rectilinear motion is equal to the increase in momentum.*

$$\int P\, dt = m\, v - m\, v_o$$

or

$$P = \frac{d\,(m\,v)}{d\,t} = \frac{d\,m}{d\,t}\, v.$$

In front of the wing, with reference to the portion $l\,dy$,

$$\frac{dm_o}{d\,t}\, v_o = (\rho\, l\, dy\, v_o)\, v_o = \rho\, l\, v_o^2\, dy \left[\frac{kg/s^2}{m^4}\, m\, \frac{m^2}{s^2}\, m = kg\right].$$

Behind the wing, $\frac{dm_1}{d\,t}\, v_1 = (\rho\, l\, dy\, v_1)\, v_1 = \rho\, l\, v_1^2\, dy\ [kg]$.

The variation in the momentum is

$$\rho\, l \int_{-\infty}^{+\infty} (v_o^2 - v_1^2)\, dy.$$

The force exerted on a section of the body, of the length l, is then

$$W = l \int_{-\infty}^{+\infty} [(p_{st_o} - p_{st_1}) + \rho\, (v_o^2 - v_1^2)]\, dy.$$

If we put

$$p_{g_o} = p_{st_o} + \frac{\rho}{2}\, v_o^2$$

and

$$p_{g_1} = p_{st_1} + \frac{\rho}{2}\, v_1^2,$$

*A. Föppl, "Einführung in die Mechanik," p. 49.

then, $W = l \int (p_{g_o} - p_{g_1})\, dy + \frac{\rho}{2} \int_{-\infty}^{+\infty} (v_o^2 - v_1^2)\, dy = J_I + J_{II}$.

The integral J_I can be easily determined, as it need not be extended to infinity, since p_{g_o} differs from p_{g_1} only within a very limited region. The integration is required only in the vortical region behind the body. The integrand vanishes, when $p_{g_o} = p_{g_1}$.

The integral J_{II} cannot be determined without being first transformed. A potential flow is assumed, which, outside of the vortical region, is identical with the flow producing the drag. Let the velocity of the potential flow be v'. Then $v_o' = v_o$ in front of the body, while behind the body, but outside of the vortical region, $v' = v_1$, whereas in the vortical region it must be assumed that $v' > v_1$, to make up for the loss of pressure. In order to account for the increase of velocity, we must assume a source, whose yield, for the above section of the body, is

$$E = l \int (v' - v_1)\, dy.$$

The assumption of a source necessitates a negative drag,

$$W' = - \rho\, v_\infty\, E$$

(v_∞ infinite velocity) similar to the Kutta and Joukowsky equation,

$$A = \rho\, v\, \Gamma\, l$$

(A = lift, ρ = density, Γ = circulation).

In the assumed potential flow, there is likewise

$$p_{g'} = p_{st_1} + \frac{\rho}{2} v'^2 = p_{g_o}.$$

Whence

$$W' = -\rho v_\infty E = l \int \underbrace{(p_{g_o} - p_{g'})}_{=0} dy + \frac{\rho}{2} l \int_{-\infty}^{+\infty} v_o^2 - v'^2) dy$$

$$W - W' = W + \rho v_\infty E = l \int (p_{g_o} - p_{g_1}) dy + \frac{\rho}{2} l \int (v'^2 - v_1^2) dy.$$

After substituting the value of the yield,

$$E = l \int (v' - v_1) dy$$

the following expression is obtained:

$$W = l \int (p_{g_o} - p_{g_1}) dy +$$

$$+ \frac{\rho}{2} l \int (v'^2 - v_1^2) dy - \rho v_\infty l \int (v' - v_1) dy =$$

$$= l \int (p_{g_o} - p_{g_1}) dy - \frac{\rho}{2} l \int (v' - v_1) (2v_\infty - (v' + v_1)) dy.$$

After this transformation, the second integral need not be extended beyond the vortical region since, outside of it, $(v' - v_1) = 0$ and the integral vanishes. Provided the front measuring point is very far from the wing, as was the case in the Gottingen wind tunnel, we can put, with sufficient accuracy,

$$v_\infty = v_o.$$

Hence,

$$W = l \int (p_{g_o} - p_{g_1}) dy - \frac{\rho}{2} l \int (v' - v_1) [2v_o - (v' + v_1)] dy.$$

In tests on an airplane in flight, constructional consider-

ations prevented placing the front measuring point in the domain of undisturbed flow. As shown in IV, this point was taken into consideration by introducing a correction factor for the velocity, this factor being determined through calibration.

Point 2.- Since the loss of energy is to be measured on a wing, the above assumption, that the lift = 0, is not correct. The wing produces lift, and in addition to the horizontal-velocity component v_1, the air behind the wing has also a vertical component w_1. Hence,

$$p_{g_1} = p_{st_1} + \frac{\rho}{2}(v_1^2 + w_1^2)$$

and

$$p_{g_o} = p_{st_o} + \frac{\rho}{2} v_o^2$$

$$W = l \int_{-\infty}^{+\infty} [(p_{g_o} - p_{st_1}) + \rho (v_o^2 - v_1^2)] \, dy =$$

$$= l \int (p_{g_o} - p_{g_1}) \, dy + \frac{\rho}{2} l \int_{-\infty}^{+\infty} (v_o^2 - v_1^2 + w_1^2) \, dy.$$

Assuming again a potential flow with a source and the yield

$$E = l \int (v' - v_1) \, dy,$$

or, more accurately,

$$l \int (\sqrt{v'^2 + w_1^2} - \sqrt{v_1^2 + w_1^2}) \, dy,$$

such a potential flow, with a downward velocity, produces the induced drag W_i. Since w did not change, the lift also remained the same.

W_i is likewise the same in both cases.

Under the influence of the source,

$$W' = W_i - \rho\, v_\infty\, E = \frac{\rho}{2}\, l \int_{-\infty}^{+\infty} (v_o^2 - v'^2 + w_1^2)\, dy$$

$$W - W_i = W_{Pr} =$$

$$-\rho\, v_\infty\, l \int (v'-v_1)dy + l \int (p_{g_o}-p_{g_1})dy + \frac{\rho}{2}\, l \int (v'^2-v_1^2)\, dy$$

$$\underline{W_{Pr} = l \int (p_{g_o} - p_{g_1})\, dy - \frac{\rho}{2}\, l \int (v' - v_1)\, (2v_o - [v' + v_1])\, dy.}$$

The result is therefore identical with that obtained in Point 1.

Point 3.- Order of magnitude of the second integral.- Since the determination of the second integral is rather complicated, an approximation method is used by estimating the share of the second integral in the first integral.

The farther the measuring point gets behind the wing, the smaller are the differences between p_{g_o} and p_{g_1} and between p_{st_o} and p_{st_1}. On the assumption that $v' \approx v_\infty$, we can write

$$\frac{v_\infty - v_1}{v_\infty} \approx \frac{p_{g_o} - p_{g_1}}{2\,\frac{\rho}{2}\, v_\infty^2}$$

since

$$\frac{p_{g_o} - p_{g_1}}{2\,\frac{\rho}{2}\, v_\infty^2} = \frac{p_{st_\infty} + \frac{\rho}{2}\, v_\infty^2 - p_{st_1} - \frac{\rho}{2}\, v_1^2}{2\,\frac{\rho}{2}\, v_\infty^2} =$$

$$= \frac{\overbrace{p_{st_\infty} - p_{st_1}}^{=\,0} + \frac{\rho}{2}\, (v_\infty^2 - v_1^2)}{2\,\frac{\rho}{2}\, v_\infty^2} = \frac{(v_\infty + v_1)\, (v_\infty - v_1)}{2v_\infty^2}$$

If we write

$$v_\infty + v_1 = v_\infty + v_\infty - (v_\infty - v_1),$$

then

$$\frac{p_{g_o} - p_{g_1}}{2\,\frac{\rho}{2}\,v_\infty^2} = \frac{[v_\infty + v_\infty - (v_\infty - v_1)]\,(v_\infty - v_1)}{2v_\infty^2} =$$

$$= \frac{2v_\infty\,(v_\infty - v_1) - (v_\infty - v_1)^2}{2v_\infty^2}.$$

The order of magnitude of $(v_\infty - v_1)^2$ is negligible against

$$2v_\infty\,(v_\infty - v_1).$$

Hence

$$\underline{\underline{\frac{p_{g_o} - p_{g_1}}{2\,\frac{\rho}{2}\,v_\infty^2}}} = \frac{2\,v_\infty\,(v_\infty - v_1)}{2\,v_\infty^2} = \underline{\underline{\frac{v_\infty - v_1}{v_\infty}}}$$

Thus the integrand of the second integral becomes

$$-\frac{\rho}{2}\,(v_\infty - v_1)\,(v_\infty - v_1) = \frac{(p_{g_o} - p_{g_1})^2}{4\,\frac{\rho}{2}\,v_\infty^2}$$

so that, in the ratio

$$\frac{p_{g_o} - p_{g_1}}{4\,\frac{\rho}{2}\,v_\infty^2},$$

it is smaller than the integrand of the first integral.

Consequently, the influence of the second integral is very small when the measuring point lies at a sufficient distance behind the wing. This distance should be so large that the difference $(p_{g_o} - p_{g_1})$ would still be within the range of accurate measurement.

II. Reynolds Law

The great importance of tests on aircraft in flight is chiefly evidenced by Reynold's Law. If the air flows, past geometrically similar wings, were perfectly similar for both the model and the actual wing, then full-scale measurements could be dispensed with. It follows from the theory, that the flow is similar, when the ratio of the inertia effects to the viscosity effects on the airfoil is the same in the wind tunnel and in a free air stream.* Hence

$$\frac{\text{Force of inertia}}{\text{Force of viscosity}} = \frac{m\, b}{\eta \frac{\partial v}{\partial n} f} = \frac{\rho\, \text{vol}\, b}{\eta \frac{1}{t} l^2} =$$

$$= \frac{\rho\, l^4/t^2}{\eta\, l^2/t^2} = \frac{\rho\, l^2}{\eta\, t} = \frac{l^2}{\frac{\eta}{\rho}\, t} = \frac{l}{t}\frac{l}{\frac{\eta}{\rho}} =$$

$$= \frac{v\, l}{\nu} = R.$$

From this simple transformation, it follows that the product of velocity times length (wing chord) divided by $\nu = \frac{\eta}{\rho}$ (kinetic viscosity) must always remain constant for comparative measurements.

The constant R is designated as "Reynolds Number." If the tests are carried out at the same kinetic viscosity, we may also write:

$$v\, l = \text{constant} = E.$$

If v is measured in m/s and l in mm, then E denotes

*Prandtl, "Ergebnisse der Aerodynamischen Versuchsanstalt zu Göttingen," Report I, p. 33.

the index value. At 760 mm and 13° C., $\nu_o = 0.143$. In this case $E = \frac{R}{70}$.

Reynolds Numbers of 200,000 to 500,000 were obtained in normal model tests for a wing chord of 20 cm, while for a wing chord of 60 cm, tested between walls, the values ranged from 600,000 to 1,500,000.

Reynolds Numbers of approximately

$$R = \frac{4000 \times 200}{0.14} \cong 6,000,000$$

were obtained in tests on an airplane in flight.

Strictly speaking, tests on models cannot be converted, as we are unable to increase the air velocity for models in the proportion specified by Reynolds law, owing to the development of new forms of flow, when the velocity of sound is exceeded.

It has been actually determined that the critical Reynolds Number of all streamlined bodies is so small that it does not lie between the measurement on the model and on the full-sized airplane (Fuchs-Hoff, "Aerodynamik").

Since, however, the drag coefficient is a function of the Reynolds Number, it is evident that the curve obtained by plotting c_w against R is continuous, but its course is not known. The importance of the Betz method is now apparent, in that the measurements can be made on full-sized aircraft.

Another method was adopted by the Americans for the purpose of obtaining a larger Reynolds Number. They have built a wind

tunnel in which a pressure of 20 atmospheres is reached. ν is reduced by increasing ρ and hence $R = \frac{v\,l}{\nu}$ is increased. As a result of these tests, Reynolds Numbers up to $R = 3{,}500{,}000$ have already been obtained.

In the general summary (p. 44) of this treatise, the above tests are more closely considered and compared with the results of the present experiments.

III. Wind-Tunnel Tests

1. Wing Section

The cantilever wing of the Junkers all-metal, postal airplane, type A 20, has a thick wing section tapering toward the tips. The wing chord also decreases toward the tips. The dimensions are given in Figs. 1 and 2. The aspect ratio is

$$\frac{F}{b^2} = 1 : 7.88 \qquad \left(\frac{b^2}{F} = 7.88 \text{ in English}\right)$$

The aerodynamical properties and the comparatively wide range of useful applications of this thick section is illustrated by the polar in Fig. 3, which was obtained from measurements in the Göttingen wind tunnel. For the wind-tunnel tests a geometrically similar model, reduced to 0.085 of the actual wing, was made of gypsum according to the Göttingen method.* The corrugated sheet ribs were omitted and the surface of the wing model was made perfectly smooth.

*"Ergebnisse der Aerodynamischen Versuchsanstalt zu Göttingen." Report I. The Construction of the Models. p. 46 ff.

3. Arrangement of Test

No serious technical difficulties were encountered in determining the energy loss by means of model measurements in the large Göttingen wind tunnel. The inverted wing model was attached to the wires of the Göttingen three-component balance.*

A Pitot tube was mounted at a certain distance in front of the model, precautions being taken that the air flow around the model should not be disturbed by the tube. A horizontally and vertically adjustable Pitot tube was arranged behind the wing. The distance from the trailing edge of the wing was determined by preliminary tests. In order to insure accurate measurement of the vertical displacement, the distance should be sufficient to leave enough space for the vortical region. On the other hand, the distance should not be too large, as, although it increases the vortical region in the vertical direction, it may reduce the accuracy of the measurements of the now decreasing pressure differences. These limits being taken into consideration, the resulting distances from the displacement line to the trailing edge of the wing are shown in Fig. 9.

The performance of the model tests was facilitated by the fact that R. Seiferth, Göttingen, had already made drag measurements on a Rohrbach wing model of 60 cm chord according to the Betz method. The results of these measurements have not yet

*"Ergebnisse der Aerodynamischen Versuchsanstalt zu Göttingen." Report I. The Three-Component Balance, p. 27 ff.

been published. The test arrangement was photographed in the wind tunnel and is shown in Figs. 4 and 5.

3. Instruments and Their Calibration

The total pressure of the steady flow was measured with a Pitot tube having a calibration factor of 1.

At the suggestion of Betz, the total pressure of the flow in the vortical region was measured with a Pitot tube which was surrounded by a Venturi tube. This instrument has a very large angular range of accurate indications, owing to the directing effect of the Venturi tube. After calibration, the correction factor to $\pm 20^\circ$ was actually 1. Errors are thus avoided, such as might otherwise result from the deflection of the flow by a lift-producing wing, if the Pitot tube had angular sensitivity.

The static pressure behind the wing, which must be known for the calculation of the velocities v_1 and v', was determined by means of a bent tube. All attempts to reduce the angular sensitivity of such instruments, for the determination of the static pressure in the same proportion as for the total pressure, have hitherto failed. The deflections were measured for the following angles (measured at the impact pressure of 58.6 kg/m^2):

β =	20°	10°	5°	0°	-5°	-10°	-20°
p_{stat} =	- 5.8	-1.2	0	+0.1	-0.3	-2.0	-7.1

The mean values of the deflections are 2% for 10° and 11%

for 20°. Deflections exceeding 10 to 15° are not likely to occur. The errors are in this case confined to the correction member (second integral), which represents only a small fraction of the total value (see 3- Instruments and Their Calibration)/ p.16. Hence the error becomes negligibly small in the final result.

4. Determination of the Polar Curve.

The polar of the wing model and the moment curve were determined in the usual way. The section is a genuine Junkers type and its polar has therefore not been published in the Göttingen reports. Still the section and the polar are similar to some of the Göttingen sections (Fig. 3). The value of the wing chord (t = 0.1893) is that of the maximum chord at the wing center.

5. Velocity Series (Influence of the Index Value)

The wing-section drag for three different angles of attack was calculated from force measurements on the wing model, over the region covered under these conditions by the Reynolds Numbers, by deducting the induced drag. The obtained values of the drag are plotted in Fig. 6 and show the expected decrease for increasing Reynolds Numbers.

6. Profile-Drag Measurements According to Betz

From I, last part of Point 1, we have

$$W_{Fr} = l \int (p_{g_o} - p_{g_1})\, dy - \frac{\rho}{2} l \int (v' - v_1)\,[2v_o - (v' + v_1)]\, dy.$$

The trajectory of the vertical displacement dy is plotted on a scale attached to the rear Pitot tube and can be read in mm.

In the tables the displacement trajectories are denoted by h (mm). Thereby the point of intersection of the chord of each wing section with the plane of displacement of the Pitot tubes is considered as the zero point of the displacement line. Direct readings of the difference between the total pressures $(p_{g_o}' - p_{g_1}')$ were taken in mm on the alcohol column of the pressure gauge (manometer). $(p_{g_o} - p_{g_1}) = 0.798.\ (p_{g_o}' - p_{g_1}')$ kg/m², s = 0.798 being the specific gravity of the alcohol. Besides, the total pressure in front of the wing (p_{g_o}') was measured and reduced to $p_{g_o} = 0.798\ p_{g_o}'$ kg/m². From a comparison with the impact pressure measured in the experiment chamber of the wind tunnel (the entrance-cone factor being taken into consideration) it appeared that the total pressure could be set equal to the impact pressure q_o.

Furthermore, the static pressure p_{st_1}' behind the wing was measured and reduced to $p_{st_1} = 0.802\ p_{st_1}'$ (kg/m²) the specific weight of the alcohol in this pressure gauge being s = 0.802. The velocity of the assumed potential flow in the

vortical region is then

$$v' = \sqrt{\frac{2}{\rho}(p_{g_o} - p_{st_1})}, \quad \text{as} \quad q' = (p_{g_o} - p_{st_1}).$$

Furthermore,

$$v_1 = \sqrt{\frac{2}{\rho}[(p_{g_o} - p_{st_1}) - (p_{g_o} - p_{g_1})]},$$

since

$$q_1 = p_{g_o} - (p_{g_o} - p_{g_1}) - p_{st_1}.$$

Likewise, we find

$$v_o = \sqrt{\frac{2}{\rho} q_o}, \quad \text{since} \quad p_{g_o} = q_o.$$

Thus the loss of pressure

$$\Delta p = (p_{g_o} - p_{g_1}) - \frac{\rho}{2}(v' - v_1)[2 v_o - (v' + v_1)]$$

for each point behind the wing can be expressed in kg/m^2.

If the loss of pressure is divided by the corresponding impact pressure (q_o) of the undisturbed flow and if $\frac{\Delta p}{q_o}$ is plotted against the different positions of h (mm), then

$$\frac{W_{Pr}}{q_o} = c_{w_{Pr}} F = l \int \frac{\Delta p}{q_o} dy.$$

The value of

$$\int \frac{\Delta p}{q_o} dy = J$$

is easily determined by planimetry.

The profile drag, which in the figures is usually designated by c_w, is then

$$c_{w_{Pr}} = \frac{l \int \frac{\Delta p}{q_o} dy}{l\ t} = \frac{J}{t}\left[\frac{m}{m}\right].$$

a) Measurements on Three Wing Sections for Four Different Angles of Attack, the Velocity Remaining the Same

These measurements were first made on three wing sections, I, II, and III, their position being shown in Fig. 9. Unfortunately, these sections could not be regularly distributed over half of the span, as the suspension device had to be taken into consideration.

The velocity was kept constant and the wing-section-drag coefficient determined for each section, i.e., for $\alpha = +8.5^{\circ}$, $+4.5^{\circ}$, $+0.8^{\circ}$, and -3.1° (angle of attack). The values obtained from the tests and calculated according to the Betz formula, for position I and $\alpha = 8.5^{\circ}$, are given in Table I.

In the same way, tables have been worked out for the values obtained from tests at the other angles of attack and for other sections. The calculated values of $\frac{\Delta p}{q_o}$ were plotted. The curves, from which $c_{w_{Pr}}$ was obtained by planimetry, are shown in Fig. 7 for position I.

In Fig. 8 the section-drag coefficient was then plotted in the usual way (without the induced drag) against the lift coefficient for sections I, II, and III, and for the four angles of attack.

The distribution of the section drag over the span is shown in Fig. 9. It corresponds roughly to the ratio of wing thickness to chord, which decreases toward the wing tips.

b) Measurements on a Wing Section for One Angle of Attack and Four Different Velocities

These measurements were made with section I at an angle of attack $\alpha = 0.8^{\circ}$ and velocities of 10, 20, 30, and 40 m/s (Fig. 10).

TABLE I. Position 1. $\alpha=+9^{\circ}$, $\varphi=0.5$: $\underline{\alpha=+8.5^{\circ}}$ s(alcohol)=0.803,

$q=58.6$ mm H_2O $\left.\begin{matrix} B=760 \\ t=18^{\circ} \end{matrix}\right\} \underline{\rho=0.1232}$ $\left[\frac{kg\ s^2}{m^4}\right]$

	1	2	3	4	5	6	7	8
	q_o''	h	$p_{g_o}'-p_{g_1}'$	p_{st_1}'	p_{g_o}'	s=0.798		s = 0.802
						$p_{g_o}-p_{g_1}$	$p_{g_o}=q_o$	p_{st_1}
	mm Alcohol	mm	mm Alcohol column			kg/m²	kg/m²	kg/m²
(a)	70.2	15	0	3.75	73.2	0	58.5	3.01
(b)	70.2	10	0	3.55	73.2	0	58.5	2.84
(c)	70.2	5	1.35	3.0	73.2	1.08	58.5	2.40
(d)	70.2	2.5	5.6	2.7	73.2	4.47	58.5	2.16
(e)	70.2	0	13.7	2.6	73.2	10.92	58.5	2.08
(f)	70.2	- 2.5	20.7	2.4	73.2	16.55	58.5	1.92
(g)	70.2	- 5.0	23.1	2.35	73.2	18.45	58.5	1.88
(h)	70.2	- 6.0	22.3	2.4	73.2	17.72	58.5	1.92
(i)	70.2	- 7.5	19.0	2.4	73.2	15.18	58.5	1.92
(j)	70.2	-10.0	11.5	2.45	73.2	9.18	58.5	1.96
(k)	70.2	-15.0	0.75	2.6	73.2	0.60	58.5	2.08
(l)	70.2	-20.0	0	2.55	73.2	0	58.5	2.04
(m)	70.2	-25.0	0	2.3	73.2	0	58.5	1.84

Table I (Cont.)

Position 1. $\alpha=+9^{\circ}$, $\varphi=0.5$: $\underline{\alpha=+8.5^{\circ}}$ s(alcohol)=0.803,

$q=58.6$ mm H_2O $\left.\begin{matrix}B=760\\t=18^{\circ}\end{matrix}\right\}$ $\underline{\underline{\rho=0.1232}}$ $\left[\frac{kg\ s^2}{m^4}\right]$

	9 $q'=p_{g_o}-p_{st_1}$ kg/m²	10 $q_1=(p_{g_o}-p_{st_1})-(p_{g_o}-p_{g_1})$ kg/m²	11 $v_1=\sqrt{\frac{2q_1}{\rho}}$ m/s	12 $v'=\sqrt{\frac{2q'}{\rho}}$ m/s	13 $v_o=\sqrt{\frac{2q_o}{\rho}}$ m/s	14 $v'-v_1$ m/s	15 $v'+v_1$ m/s
(a)	55.49	55.49	30.01	30.01	30.8	0	60.02
(b)	55.66	55.66	30.04	30.04	30.8	0	60.08
(c)	56.10	55.02	29.90	30.18	30.8	0.28	60.08
(d)	56.34	51.87	29.00	30.23	30.8	1.23	59.23
(e)	56.42	45.50	27.18	30.28	30.8	3.10	57.46
(f)	56.58	40.03	25.50	30.30	30.8	4.8	55.80
(g)	56.62	38.17	24.90	30.30	30.8	5.4	55.20
(h)	56.58	38.86	25.11	30.30	30.8	5.19	55.41
(i)	56.58	41.40	27.91	30.30	30.8	4.29	56.21
(j)	56.54	47.36	27.72	30.29	30.8	2.57	58.01
(k)	56.42	55.82	30.10	30.28	30.8	0.18	60.38
(l)	56.46	56.46	30.25	30.25	30.8	0	60.50
(m)	56.66	56.66	30.30	30.30	30.8	0	60.60

Table I (Cont.)

Position 1. $\alpha=+9^{\circ}$, $\varphi=0.5$: $\underline{\alpha=+8.5^{\circ}}$ s(alcohol)=0.803,

$q=58.6$ mm H_2O $\left.\begin{matrix} B=760 \\ t=18^{\circ} \end{matrix}\right\}$ $\underline{\underline{\rho=0.1232}}$ $\left[\frac{kg\ s^2}{m^4}\right]$

	16 $2v_o-(v'+v_1)$ m/s	17 $\frac{\rho}{2}(v'-v_1)[2v_o-(v'+v_1)]$ kg/m²	18 $\Delta p=(p_{g_o}-p_{g_1})-\frac{\rho}{2}(\ldots)(\ldots)$ kg/m²	19 $\frac{\Delta p}{q_o}$
(a)	1.58	0	0	0
(b)	1.52	0	0	0
(c)	1.52	0.026	1.05	0.018
(d)	2.37	0.18	4.29	0.073
(e)	4.14	0.79	10.13	0.173
(f)	5.80	1.72	14.83	0.254
(g)	6.40	2.13	16.32	0.279
(h)	6.19	1.98	15.74	0.269
(i)	5.39	1.428	13.75	0.235
(j)	3.59	0.854	8.33	0.142
(k)	1.22	0.015	0.58	0.0099
(l)	1.10	0	0	0
(m)	1.00	0	0	0

The dash line in Fig. 6 represents the profile-drag values obtained from Fig. 10 by planimetry and plotted against the Reynolds Number. The curve is identical with the drag curve determined by means of the wind-tunnel balance. In this case, however, the dependence of $C_{w_{Pr}}$ on R is only given over a very small range (up to R = 450,000). The further development of this curve $C_{w_{Pr}} = f(R)$ must be determined by full-scale measurements on an airplane in flight.

6. Summary

In order to enable a comparison of the two methods

a) $C_{w_{Pr}} = C_{w\ total} - C_{w_i}$ and

b) $C_{w_{Pr}} = \frac{J}{t}$,

it was attempted to calculate a mean value for the whole wing from the values determined by the Betz method for different wing sections. However, attention must be called to the fact that this mean value cannot be accurate, since it is obtained from only three wing sections, irregularly distributed along the span. It was found that

$$W_{Pr} = C_{w_{Pr}}\, q\, F$$

$$= q\,(C_{w_I} F_I + C_{w_{II}} F_{II} + C_{w_{III}} F_{III}$$

$$= q\, C_{w_{Pr}} \Sigma F$$

$$C_{wPr} = 100\, C_{wPr}$$

$$F_I = 0.1030\ m^2; \quad F_{II} = 0.0432\ m^2; \quad F_{III} = 0.0635\ m^2;$$

$$\Sigma F = 0.2097\ m^2 .$$

TABLE II

α^o	C_{w_I}	$C_{w_I}F_I$	$C_{w_{II}}$	$C_{w_{II}}F_{II}$	$C_{w_{III}}$	$C_{w_{III}}F_{III}$	$\Sigma(C_w F)$	$C_{w_m} = \frac{\Sigma (C_w F)}{\Sigma F}$
-3.1	1.290	0.134	1.233	0.0531	1.101	0.0661	0.2532	1.221
0.8	1.250	0.130	1.098	0.4742	0.954	0.0572	0.2344	1.132
4.5	1.403	0.146	1.440	0.0620	1.145	0.0687	0.2767	1.340
8.5	1.755	0.183	1.855	0.0796	1.351	0.0811	0.3432	1.660

The mean wing-section-drag coefficients obtained from the last column of the above table were plotted in Fig. 11 against the lift coefficient (curve a). The values of the differences for the wing-section drag of the whole wing computed from the polar curve (Fig. 3) were also plotted in this diagram for comparison.

The directions of both curves are similar. It appears, however, that the values measured by the momentum method are smaller than those determined by force measurements, for lift values exceeding 0.75. Since the total drag values determined by force measurements are likely to be correct, owing to the great experience gained with this method, we must assume, either that the values obtained with momentum measurements are too small or that the actual induced drag is higher than the theoretically calculated induced drag. The writer believes the second assumption to be the more reasonable one.

It is shown that the Betz method can be successfully applied to model tests and that it is comparatively easy to use. In addition to this fact, it has the advantage of being more accurate.

IV. Tests on an Airplane in Flight

1. Airplane and Engine

Built by: Junkers-Flugzeugwerke A.-G., at Dessau.

Type: All-metal postal airplane; type A 20-land; D 708 (Fig. 12).

Position and number of wings: Enbraced, cantilever, tapered (thickness and chord), low-wing monoplane.

Occupants: 1 pilot, 1 passenger.

Propeller: 1 tractor propeller (axis above wing); direct drive; diameter, 2.9 m (9.5 ft.); pitch, 2.5 m (8.2 ft.).

Main dimensions: Span, 15.27 m (50.1 ft.), total length, 8.3 m (27.3 ft.), height, 2.95 m (9.7 ft.).

Wing area and weights:

Wing area	30.5	m^2	(328.3 sq.ft.)
Weight empty	960	kg	(2116.4 lb.)
Useful load	540	"	(1190.5 ")
Engine: B.M.W. IV	240	HP	
Wing loading	49	kg/m^2	(10 lb./sq.ft.)
Power "	6.5	kg/HP	(14.1 lb./HP.)
Total weight	1500	kg	(3306.9 lb.)

2. Testing Mechanism

Although the installation of the testing mechanism in the wind tunnel was very easy, considerable difficulty was experienced in mounting it on the airplane. The constructional solution for securing it on the wing was rendered more difficult by the fact that the wing could not be damaged, nor the flow around the wing remain changed, nor the flying properties of the airplane be impaired. The protection of the testing mechanism against vibrations was found to constitute another difficulty.

The testing mechanism was designed by the writer who received valuable assistance and advice from the Junkers laboratory and the D.V.L. ("Deutsche Versuchsanstalt für Luftfahrt"). The mechanism was prepared in a very short time in the D.V.L. workshops.

a) The Installation in Front of the Wing

The pressure gauges in front of the wing must be placed in a steady flow.* Considerable experience had been gained by the D.V.L. on this subject during the previous year's Lillienthal contest. Consequently, the instruments were installed by the physical section of the D.V.L. A Prandtl, a Brabbée, and a D.V.L. pressure tube were secured in front of the wing. The junction point of the three instruments was covered by a fairing. From this point pipes were run to an instrument board in the fuselage. Structural details are shown in Figs. 13 and 14. As regards Fig. 14, it should be noted that, after the photograph

*Ahlborn, "Orte fur die Messgerate an Flugzeugen." Positions for Instruments on Airplanes. "Z.F.M." 1925, No. 1.

had been taken, the junction point was braced against both the leading and the trailing edge of the wing.

In order not to affect the flow around the wing, the pressure gauges were mounted on the left wing, whereas the main testing apparatus was installed behind the right wing. In order to obtain accurate measurements, the instruments were placed outside the propeller slip stream. q_∞ was measured with the front Pitot tube and the readings were corrected by a factor calculated from speed flights. As in the case of wind-tunnel tests, the assumption that $p_{g_o} = q_o = q_\infty$ is admissible, owing to the fact that the impact pressure of the undisturbed flow is recorded by the front Pitot tube (a calibration factor being used) and that the dynamic pressure of the undisturbed flow is measured by a sounding device. The correction factor varies, however, with the circulation. In this case, however, the effect seems to be negligible, since the tests are made within a small speed range (1 : 1.33).

The D.V.L. tube operated a triple recording instrument. However, the diagrams plotted by this instrument were not required for these tests.

b) Installation Behind Right Wing

A T-section steel rail was fastened to a steel tube, which ran parallel to the trailing edge of the right wing about a meter behind it. A slide, running on the tail, carried two in-

struments, a Prandtl and a Brabbée pressure tube. The slide could be moved up and down from the pilot's cockpit by means of a cable. A pointer attached to the slide moved up and down a fixed scale, graduated in centimeters, which could be accurately read from the observer's cockpit. The T-rail, together with the two instruments, could be tipped over and then be returned to the vertical position by the observer after the take-off. Before landing, the rail had to be tipped over again, in order to prevent it from striking the ground. A large thermometer, which could also be read from the cockpit, was fixed to the brace rod. Other details and the bracing of the mechanism are shown in Figs. 15-17. The mechanism is secured to the trailing edge by means of a large piece of aluminum.

In spite of the difficulties of this installation, the original plan to use several superposed fixed tubes instead of a movable pressure gauge was abandoned, as no data were then available on the mutual interference of the propeller tubes.

c) Instrument Board

A board with alcohol manometers had already been used by Everling during the war for fin-pressure measurements on a flying airplane. Although I personally disliked the idea of using liquid manometers on a flying airplane, I had finally to adopt this method, after preliminary tests with recording instruments. The disadvantage of these instruments lies in their great sensi-

tivity to temperature changes. As only very small pressure differences were measured in this case, the recording instruments were not sensitive enough and the inertia effects of the pointers exerted considerable influence on the readings. I attempted in vain to use the Wieselsberger pressure gauge which was kindly put at my disposition by Betz and which had given good results during lift measurements made by Pröll on an airplane in flight. The range of the pointers was too small, however, and the accuracy of the measurements would have been considerably impaired.

I obtained very good results with liquid U-tubes. They could be successfully used in tests on unaccelerated airplanes and the tests in question could be flown only in calm weather. Tubes of different diameters must first be tested in flight. No damping of the vibrating liquid column was required. Five U-tubes of 6 mm diameter were used for these tests. The liquid used was red-colored alcohol. A diagram of the tube connections is shown in Fig. 18.

Manometer 1 was designed to be used in case one of the glass tubes should be broken by take-off or landing shocks. It could also be connected during flight with any of the branch pipes.

Manometer 2 showed the impact pressure in front of the wing $q_o = \frac{1}{k} q_\infty$.

Manometer 3 gave the very important value of the total pressure difference $(p_{g_o} - p_{g_1})$.

Manometer 4 was used as a check for the installation in front of the wing. A relation was established between the static pressure in front of the wing and the static pressure of the undis-

turbed flow measured by the sounding instrument. Had the installation in front of the wing been faultless, i.e., had this front point of measurement been placed in the undisturbed flow, no deflection of the manometer should have been obtained. As a matter of fact, pressure differences were observed in this case, but their numerical value was neglected in the calculations, since the correction factor had already been introduced in their stead.

Manometer 5: The static pressure of the undisturbed flow, recorded by the static sounding instrument, is compared to the static pressure behind the wing p_{st_1}.

The instrument board also carried a weight suspended by a spring. Its position of rest was indicated by a pointer. When vertical accelerations were recorded by deflections of the pointer in the photographic picture, the readings of the alcohol columns could not be used. The determination of the magnitude of the acceleration was not required. On the board there was also a liquid fore-and-aft and lateral inclinometer. The time of the measurement was recorded by a stop watch on the instrument board. The momentary position of the pointer of the pressure tubes on the graduation was marked with chalk on a black space of the board.

A camera was installed behind the observer's cockpit and could be operated from the inside of the cockpit. For the measurement, the pressure tubes were brought to a certain altitude. This position, together with the number and date of the test

were markedon the black space, whereupon about 20 pictures of this position were taken by turning the camera crank. Each time a picture was to be taken, the pilot was notified by means of a mirror. The observer had to lie down in the cockpit while a picture was being taken and the pilot had to keep the impact pressure as nearly as possible to a value previously agreed on. The instrument board installed on the airplane is shown in Fig. 19, and a portion of the film in Fig. 20.

The graduations are not clearly apparent on the photograph, but the film itself was sharper and an accurate calibration of the microscope giving readings in millimeters was possible. In some cases the readings may have been subject to error, when the liquid moistened the glass while flowing back, thus veiling the level of the alcohol column. At all events, the resulting errors may be assumed to be equal on both sides. Moreover, errors in reading are largely compensated by the fact that the final result is obtained by graphic interpolation over a series of separate pressure measurements. The readings of the values, i.e., of the liquid levels, are made from the original film by means of a microscope with an ocular scale calibrated to read the millimeter scales placed behind each manometer.

3. Instruments and Calibration

A. Instruments

a) Pressure tubes.

Owing to the fact that the direction of motion of the air on an airplane in flight never constantly coincides accurately with the axis of the tube, the main condition for a static tube is to be unsensitive to changes of direction. This is particularly the case with the Brabbée tube. As shown in Figs. 21 and 22,* the total pressure is almost perfectly recorded for inclinations of 20 to -20°.

It also appears from these two diagrams that the Brabbée tube is unsuited for impact-pressure and static-pressure measurements. In this case the Prandtl tube is better. For these reasons both a Brabbée and a Prandtl tube were installed in front of and also behind the wing.

The D.V.L. tubes could not be used because their transformation ratio was too large for the measurements in question ($q' \cong 12\ q$).

b) Static sounding device.

The datum zero-point for the static pressure behind the wing was determined by means of a sounding device, such as had already been used for airship measurements. After the take-off, the device was let down at the end of a 10-meter rubber tube. The device is streamlined and automatically assumes the wind direction.

*Air Flow Measurements by Means of Kumbruch Tubes. V.D.I., "Forschungsheft," 1921.

Details on this sounding device were published in "Zeitschrift für Flugtechnik und Motorluftschiffahrt."* The position of the static sounding device in flight is shown in Fig. 23.

c) Goerz barograph No. 19582.

This barograph was carried on all the test flights. The barograms are used for the calculation of air densities according to the well-known method.

d) Thermometer.

An ordinary liquid thermometer of large size was used for the tests and attached in a vertical position to the upper surface of the wing. Readings were taken from the observer's cockpit and written down during the flight. The observed values were supplemented by notes from the Staaken weather reports.

B. Calibration

a) Pressure tubes.

The instruments were calibrated in the Göttingen wind tunnel at different wind velocities.

1. For the Brabbée tubes I and II, the following mean correction factor was obtained:

$$\frac{p_{ges}}{q} = 0.99.$$

2. For the Prandtl tubes I and II, the following calibration factor was obtained in the same way:

$$\frac{q}{q_{eff}} = 0.99.$$

*Koppe, Measurements on Aircraft. "Z.F.M.," yearbook, 1924.

b) Impact-pressure liquid manometer calibrated through velocity measurements.

According to the well-known method, three triangular flights were made with the D 708 airplane.

1. Speed flight No. 13, on November 9, 1925.

The following values were obtained from the calculation of the flight results:

$$v = 39.5 \text{ m/s}$$

$$b_o = 736.7 \text{ mm Hg}, \quad t_o = 7^o \text{ C}.$$

From the barogram, $b = 715$ mm Hg

From the temperature curve, $t = 5.5^o$ C.

According to the Landolt-Börnstein tables, the density of the air is

$$\rho = \frac{\gamma}{g} = \frac{1.192}{9.81} = 0.1216 \frac{kg/s^2}{m^4} ;$$

and the impact pressure is

$$q = \frac{\rho}{2} v^2 = \frac{0.1216}{2} 39.5^2 = 95 \text{ kg/m}^2$$

Reading of the pressure tube:

$$h = 120 \text{ mm alcohol}.$$

For s (alcohol) = 0.81

we obtain $$q'' = 97 \text{ kg/m}^2.$$

Taking the calibration constant of the Prandtl tube B I ($\psi_1 = 0.99$) into consideration, we obtain

$$q' = \frac{97}{0.99} = 98 \text{ kg/m}^2$$

whence the installation factor is

$$\varphi_1 = \frac{q}{q'} = \frac{95}{98} = 0.97.$$

2. Speed flight No. 18, on November 11, 1925:

$$v = 45.0 \text{ m/s}$$

$b_o = 765.8$ mm; $t_o = + 10^\circ$ C.

$b = 715.0$ "; $t = - 0.5^\circ$ C.

$$\rho = \frac{\gamma}{g} = \frac{1.219}{9.81} = 0.1243 \frac{\text{kg/m}^2}{\text{m}^4}$$

$$q = \frac{\rho}{2} v^2 = \frac{0.1243}{2} \times 45^2 = 126 \text{ kg/m}^2.$$

Pressure tube:

$h = 160$ mm alcohol ($s = 0.81$)

$q'' = 130$ kg/m^2

Tube B I:

$\psi_1 = 0.99$

$$q' = \frac{130}{0.99} = 131 \text{ kg/m}^2$$

Installation factor:

$$\varphi_1 = \frac{q}{q'} = \frac{126}{131} = 0.96.$$

3. Speed flight No. 20, on November 12, 1925:

$$v = 42.0 \text{ m/s}$$

$b_o = 769.7$ mm; $t_o = 5^oC.$

$b = 710.0$ "; $t = -1.9^oC.$

$$\rho = \frac{\gamma}{g} = \frac{1.216}{9.81} = 0.1240 \frac{kg/s^2}{m^4}$$

$$q = \frac{\rho}{2} v^2 = \frac{0.1240}{2} \times 42^2 = 110 \text{ kg/m}^2.$$

Tube B I:

$\psi_1 = 0.99$

$h = 140$ mm alcohol ($s = 0.81$)

$q'' = 113$ kg/m^2

$$q' = \frac{113}{0.99} = 114 \text{ kg/m}^2$$

Installation factor:

$$\varphi_1 = \frac{q}{q'} = \frac{110}{114} = 0.97.$$

The average value adopted for the installation factor is 0.97. Hence the factor k_1, by which all the impact pressures measured in front of the wing (alcohol column) must be multiplied, is

$$k_1 = \frac{\varphi_1 s}{\psi_1} = \frac{0.97 \times 0.81}{0.99} = 0.795 \text{ (Table III, column 7)}$$

in which

φ_1 = Installation factor,

ψ_1 = Calibration constant of the Prandtl tube,

s = Specific gravity of the alcohol.

The difference of the total pressures $(p_{g_o} - p_{g_1})$ is simply and correctly recorded, the calibration constants of the two Brabbée tubes being eliminated when forming the difference. In order to obtain the pressures in millimeters of water column, the above values must be multiplied by the specific gravity of the alcohol $(s = 0.81)$.

Owing to the slight influence of the static pressure p_{st_1} behind the wing on the total result, no correction factor was determined for this value, for which a relation to the static sounding device was established. Besides, very slight changes only would be produced by this correction factor.

4. Wing-Section-Drag Measurements at Different Impact Pressures

For each series of tests, it was attempted to maintain the impact pressure as constant as possible. This condition required skillful piloting, as the A 20 is extremely sensitive in flight and responds to the slightest action of the controls. No measurements could be taken in curving flight nor in squally weather. The values measured were exactly the same as obtained in wind-tunnel tests. Only the change of the air density for the different points of measurement had to be taken into consideration.

After about 25 preliminary test flights, six main test flights were carried out. The results were summarized in six tables, one of which is Table III.

The curves in Fig. 24 were then plotted from values calculated in the same way as in the model tests.

If the difficulties of flight tests, which are certainly much greater than those of wind-tunnel tests, are taken into consideration, the results are quite satisfactory.

It should be mentioned, however, that the static-pressure measurements in flight were rather inaccurate, owing to oscillations of the sounding device. However, these inaccuracies could not substantially affect the result, since it has been mathematically established that the influence of the second integral is very small.

The fact that the longitudinal inclination of the instrument board was disregarded, entailed some inaccuracy. It can, however, be assumed that the position of the board was approximately vertical during the flights, so that the cosine of the angle of inclination was near 1. Besides, the effect of this omission is eliminated, when Δp is divided by the dynamic pressure q_o.

All the tests were made on a wing section which, owing to its distance from the fuselage axis, nearly corresponded to section I of the model. The distance of the section from the center of the fuselage was 2.680 m (8.8 ft.). At this point the wing chord was t = 2120 mm (7 ft.). This section was chosen because it was least subject to the influence of the propeller slip stream and of the rudder. The influence of the propeller

slip stream on the magnitude of the wing-section drag is therefore rather small, since the point of measurement lies at 1.1m (3.6 ft.) from the propeller disk.

As in the case of model measurements, the point of intersection of the extended wing chord with the plane of displacement which lies at a distance of 925 mm (3 ft.) behind the trailing edge was chosen as the datum zero point for the displacement paths of the pressure tubes. As a result of model tests, this distance appeared to be suitable. The total weight of the aircraft was determined by weighing. The fuel tanks were filled before each flight. In every case the total weight, including the crew, was

$$G = 1445 \text{ kg } (3186 \text{ lb.})$$

The corresponding lift values were calculated according to the formula

$$C_a = \frac{G}{F} \frac{100}{q_o}$$

TABLE III.

1	2	3	4	5	6	7	8
Time	h	$\rho=\frac{\gamma}{g}$	q_o''	$p_{g_o}''-p_{g_1}''$	p_{st_1}''	$q_o=p_{g_o}$ $=0.795$ q_o''	$p_{g_o}-p_{g_1}$ $=0.81(..)$
min.	cm	$\frac{kg/s^2}{m^4}$	mm alcohol column			kg/m²	kg/m²
3.5	+ 5	0.1245	160	0	12	127	0
	+ 5	0.1245	160	0	12	127	0
4.0	0	0.1230	160	0	30	127	0
	0	0.1230	160	0	30	127	0
4.5	- 2.5	0.1220	166	8	28	132	6.48
	- 2.5	0.1220	156	6	28	124	4.86
5.0	- 5	0.1212	170	24	24	135	19.4
	- 5	0.1212	172	22	26	137	17.8
5.5	- 7.5	0.1205	160	42	22	127	34.0
	- 7.5	0.1205	158	42	26	126	34.0
6.0	-10	0.1197	172	50	24	137	40.5
	-10	0.1197	170	52	24	135	42.1
6.5	-12.5	0.1190	160	36	28	127	29.2
	-12.5	0.1190	160	34	34	127	27.5
7.0	-15	0.1182	180	24	40	143	19.4
	-15	0.1182	160	18	28	127	14.6
7.5	-20	0.1175	166	0	30	132	0
	-20	0.1175	164	0	26	130	0
8.0	-15	0.1170	174	20	32	138	16.2
	-15	0.1170	176	16	22	140	12.9
8.5	-10	0.1165	156	48	24	124	38.9
	-10	0.1165	170	48	36	135	38.9
9.0	- 5	0.1160	160	20	22	127	16.2
	- 5	0.1160	162	18	28	129	14.6
9.5	0	0.1157	166	0	28	132	0
	0	0.1157	170	0	30	135	0
10.0	+ 5	0.1155	160	0	30	127	0
	+ 5	0.1155	164	0	28	130	0

TABLE III (Cont.)

1	9	10	11	12.	13.	14.
Time	p_{st_1} =0.81 p_{st_1}"	$q'=p_{g_o}$ $-p_{st_1}$	$q_1=(p_{g_o}-p_{st_1})$ $-(p_{g_o}-p_{g_1})$	$v'=\sqrt{\frac{2q'}{\rho}}$	$v_1=\sqrt{\frac{2q_1}{\rho}}$	$v_o=\sqrt{\frac{2q_o}{\rho}}$
min.	kg/m²	kg/m²	kg/m²	m/s	m/s	m/s
3.5	9.7	117.2	117.3	43.5	43.5	45.2
	9.7	117.2	117.3	43.5	43.5	45.2
4.0	24.2	102.6	102.8	41.0	41.0	45.5
	24.2	102.6	102.8	41.0	41.0	45.5
4.5	22.6	109.5	103.0	42.4	41.1	46.5
	22.6	101.5	96.7	40.8	39.8	45.1
5.0	19.4	115.4	96.2	43.7	39.8	47.3
	21.0	115.8	98.2	43.8	40.2	47.5
5.5	17.8	109.1	75.2	42.6	35.3	45.9
	21.0	104.8	71.0	41.8	34.5	45.7
6.0	19.4	117.4	77.1	44.4	35.8	47.9
	19.4	115.4	73.5	44.0	35.0	47.5
6.5	22.6	104.3	75.2	42.0	35.5	46.2
	27.5	99.3	72.0	41.0	34.7	46.2
7.0	32.4	110.5	91.2	43.4	39.3	49.2
	22.6	104.3	89.8	42.1	38.9	46.4
7.5	24.2	107.6	107.8	42.9	42.9	47.5
	21.0	108.8	109.0	43.1	43.1	47.1
8.0	25.9	112.0	95.9	43.9	40.5	48.6
	17.8	122.1	109.3	45.8	43.2	48.9
8.5	19.4	104.4	65.7	42.5	33.5	46.2
	29.7	105.7	67.0	42.8	33.9	48.2
9.0	17.8	109.1	93.0	43.5	40.0	46.8
	22.6	106.3	91.8	43.0	39.8	47.2
9.5	22.6	109.3	109.4	43.6	43.6	47.8
	24.2	110.6	110.8	43.9	43.9	48.4
10.0	24.2	102.6	102.8	42.2	42.2	47.0
	22.6	107.3	107.4	43.2	43.2	47.5

TABLE III (Cont.)

1	15	16	17	18	19	20
Time	$v'-v_1$	$v'+v_1$	$2v_o-(v'+v_1)$	$\frac{\rho}{2}(v'-v_1)[2v-(v'+v_1)]$	Δp	$\frac{\Delta p}{q_o}$
min.	m/s	m/s	m/s	kg/m²	kg/m²	
3.5	0	87.0	3.4	0	0	0
	0	87.0	3.4	0	0	0
4.0	0	82.0	9.0	0	0	0
	0	82.0	9.0	0	0	0
4.5	1.3	83.5	9.5	0.75	5.73	0.043
	1.0	80.6	9.6	0.58	4.28	0.035
5.0	3.9	83.5	11.1	2.64	16.76	0.124
	3.6	84.0	11.0	2.41	15.39	0.112
5.5	7.3	77.9	13.9	6.11	27.89	0.220
	7.3	76.3	15.1	6.64	27.36	0.217
6.0	8.6	80.2	15.6	8.03	32.47	0.237
	9.0	79.0	16.0	8.60	33.50	0.248
6.5	7.5	77.5	14.9	6.65	22.55	0.178
	6.3	75.7	16.7	6.26	21.24	0.168
7.0	3.1	82.7	15.7	2.88	16.52	0.116
	3.2	81.0	11.8	2.23	12.37	0.097
7.5	0	85.8	9.2	0	0	0
	0	86.2	8.0	0	0	0
8.0	3.4	84.4	12.8	2.54	13.66	0.099
	2.6	89.0	8.8	1.34	11.56	0.083
8.5	9.0	76.0	16.4	8.51	30.39	0.245
	8.9	76.7	19.7	10.1	28.8	0.213
9.0	3.5	83.5	10.1	2.05	14.15	0.111
	3.2	82.8	11.6	2.15	12.45	0.097
9.5	0	87.2	8.4	0	0	0
	0	87.8	9.0	0	0	0
10.0	0	84.4	9.6	0	0	0
	0	85.4	8.0	0	0	0

It will be remembered that none of the values was determined by readings or by means of recording instruments. They were all photographed (filmed) and accurately computed from the film with a microscope.

Summary

The wing-section-drag coefficients resulting from flight tests for different impact pressures, and the lift coefficients calculated for a small climbing and gliding angle, a constant weight of the airplane being assumed, are plotted in Fig. 25.

The curve shows the final result of the flight tests. The curve confirms the results previously obtained in model tests. The dash line represents the result of model tests (Fig. 8) and is added for comparison. The two curves are of similar shape. However, the wing-section-drag coefficients are smaller than the values measured on the model. This seems to indicate a further decrease of the wing-section drag for larger Reynolds Numbers.

It has already been pointed out that wind-tunnel model tests were carried out in America at a pressure of 20 atmospheres, whereby the Reynolds Numbers reached values of R = 3,500,000. Although the results were not obtained on a Junkers wing section (the Göttingen 387 is also a thick section), they show that there is a further decrease of the drag for Reynolds Numbers larger than those reached during the measurements in Göttingen (R = 1,000,000) - see N.A.C.A. Technical Note No. 219. Fig. 26

was computed from the American results. The drag curve for increasing Reynolds Number is similar to the curve obtained in Göttingen (Fig. 6).

The tests had to be temporarily discontinued, partly for lack of time and partly owing to damages sustained by the airplane from the high stresses exerted by the testing installation. The number of tests already completed is, however, too small for formulating definite conclusions. I was unable to proceed with the tests which I had planned before beginning this work. By using the testing installation which has been described above, I then intended to direct my investigations toward the determination of the influence of surface roughness on profile drag and to carry out profile-drag measurements behind the ailerons.

The main object of this work was to develop and test experimental apparatus for demonstrating the practical applicability of the new Betz testing method. With the experience thus gained, it will surely be possible to facilitate the performance of the tests and to lessen the inaccuracies always involved in pioneer work, so that ultimately complete experimental researches can be carried out on airplanes in flight. I think that I have at least demonstrated that work in this very recent field of research lies entirely within the realm of possibility, and also that the path to be followed lies in this field.

Bibliography

1. Aerodynamische Versuchsanstalt in Gottingen: "Berichte und Abhandlungen," I und II Lieferung, 1923.

2. Ahlborn, Orte für die Messgeräte an Flugzeugen. "Z.F.M." "Zeitschrift für Flugtechnik und Motorluftschiffahrt," 1925, Heft 1.

3. Bennewitz, Flugzeuginstrumente. Handbuch der "Flugzeugkunde," 1922.

4. Betz, Ein Verfahren zur direkten Ermittlung des Profilwiderstandes. "Z.F.M.," 1925, Heft 3.

5. Bairstow, Applied Aerodynamics, 1920.

6. Budig, Bericht über Versuche und Druckmessungen an Querrudern im Fluge. "Z.F.M.," 1925, Heft 16.

7. Everling, Ikle und Sieber, Flossendruckmessungen. "Technische Berichte" I, 6.

8. Everling und Zabel, Verhalten der Flugzeuge im Fluge. "Technische Berichte" I, 6.

9. Fuchs und Hopf, Aerodynamik. Handbuch der "Flugzeugkunde," 1922.

10. Hoff, Versuche an Doppeldeckern zur Bestimmung ihrer Eigengeschwindigkeit und Flugwinkel. "Luftfahrt und Wissenschaft" 6 Heft.

11. Koppe, Messungen an Luftfahrzeugen. "Z.F.M. Berichte und Abhandlungen," 1925, Heft 12.

12. Kröner, Versuche über Strömungen in stark erweiterten Kanalen. "Verein deutscher Ingenieure Forschungsheft," 1919.

13. Kumbruch, Messung strömender Luft mittels Staugeräten. "V.D.I. Forschungsheft," 1921.

14. Lachmann, Der Leichtflugzeugbau, 1925.

Bibliography (Cont.)

15. Landolt-Bornstein, Physikalisch-chemische Tabellen, 1923.

16. Mises, Fluglehre.

17. National Advisory Committee for Aeronautics, United States, Reports and Technical Notes.

18. Proll, Versuche am fliegenden Flugzeug. "Z.F.M.," 1921.

19. Regeln fur Leistungsversuche an Ventilatoren und Kompressoren, "V.D.I.," 1925.

20. Riefler, Tabellen der Luftgewichte, 1912.

21. Winkel, Staurohren zur Messung des Druckes und der Geschwindigkeit im fliessenden Wasser. "V.D.I.," 1923, S.568.

Translation by W. L. Koporinde, Paris Office,
National Advisory Committee
for Aeronautics.

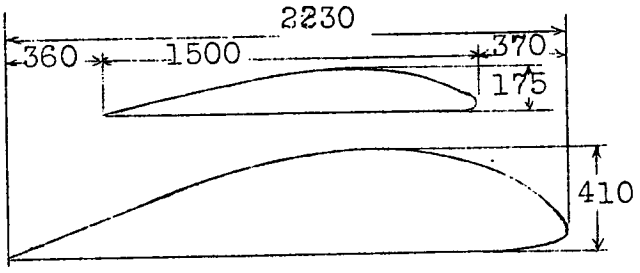

Fig.1 Wing section at root and at tip.

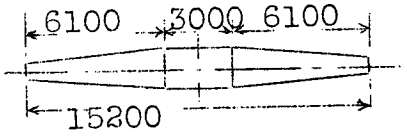

Fig.2 Wing plan

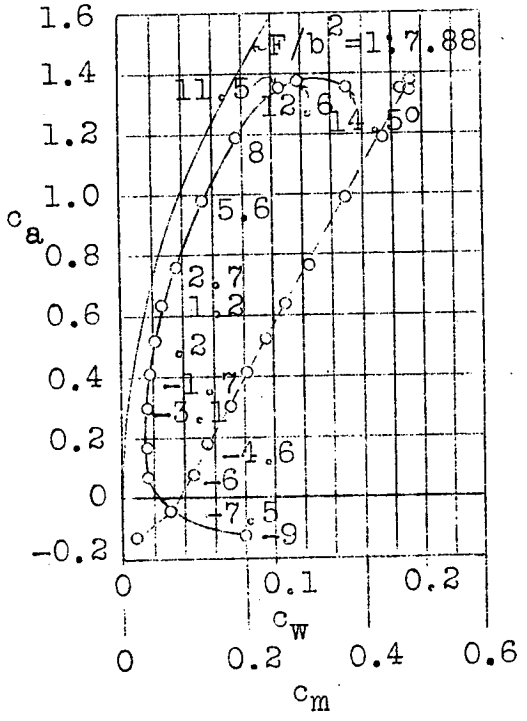

Fig.3 Polar of A20 wing.

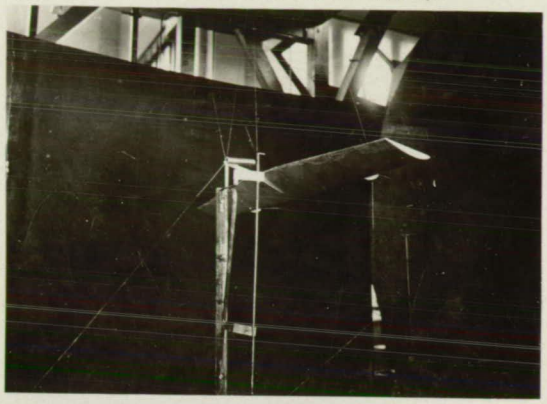

Fig.4

Fig.12 Junkers all-metal mail airplane

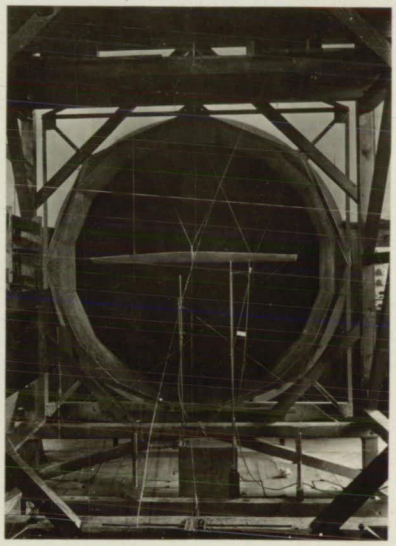

Fig.5

Fig. 16

Fig.14 Installation in front of left wing

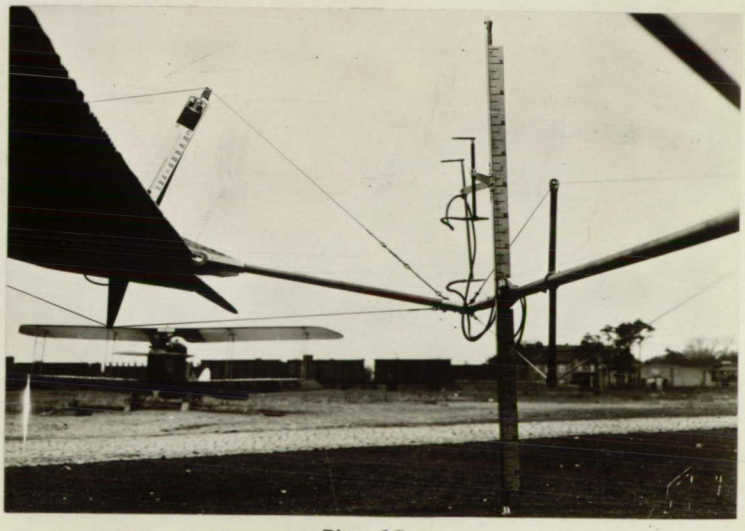

Fig. 17

– – + – – c_w by Betz method for position I of Pitot tube

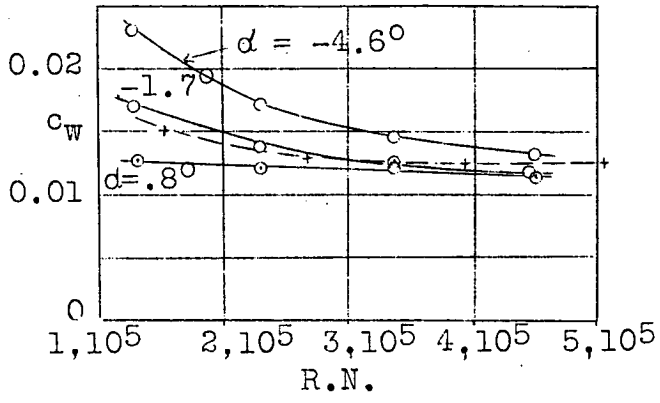

Fig.6 Profile drag plotted against Reynolds Number.

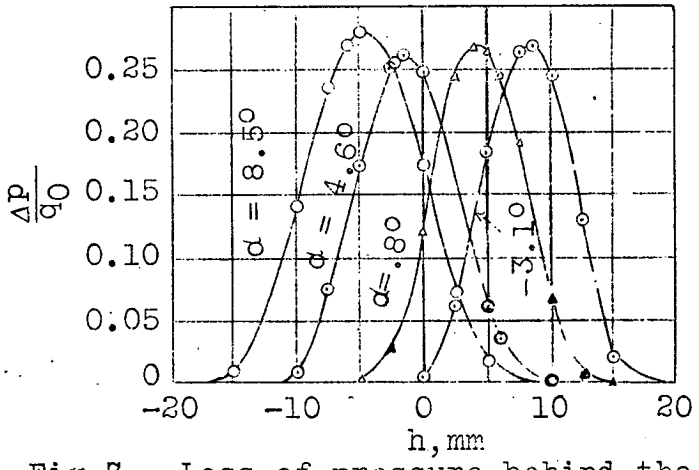

Fig.7 Loss of pressure behind the wing in position Id. Values obtained for 4 angles of attack and v = 30 m/s.

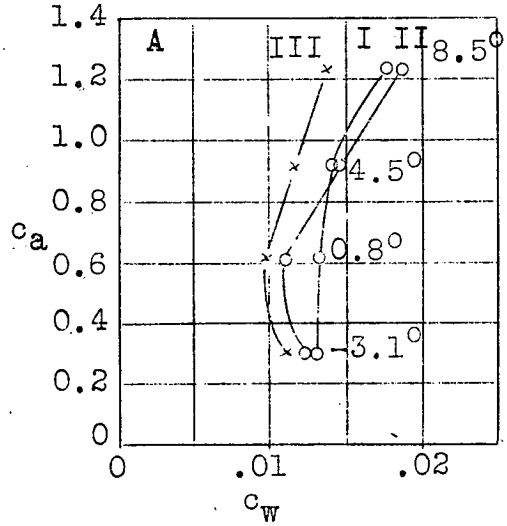

A, Position of pressure gauges

Fig.8 Section drags of the A20 wing for three different sections

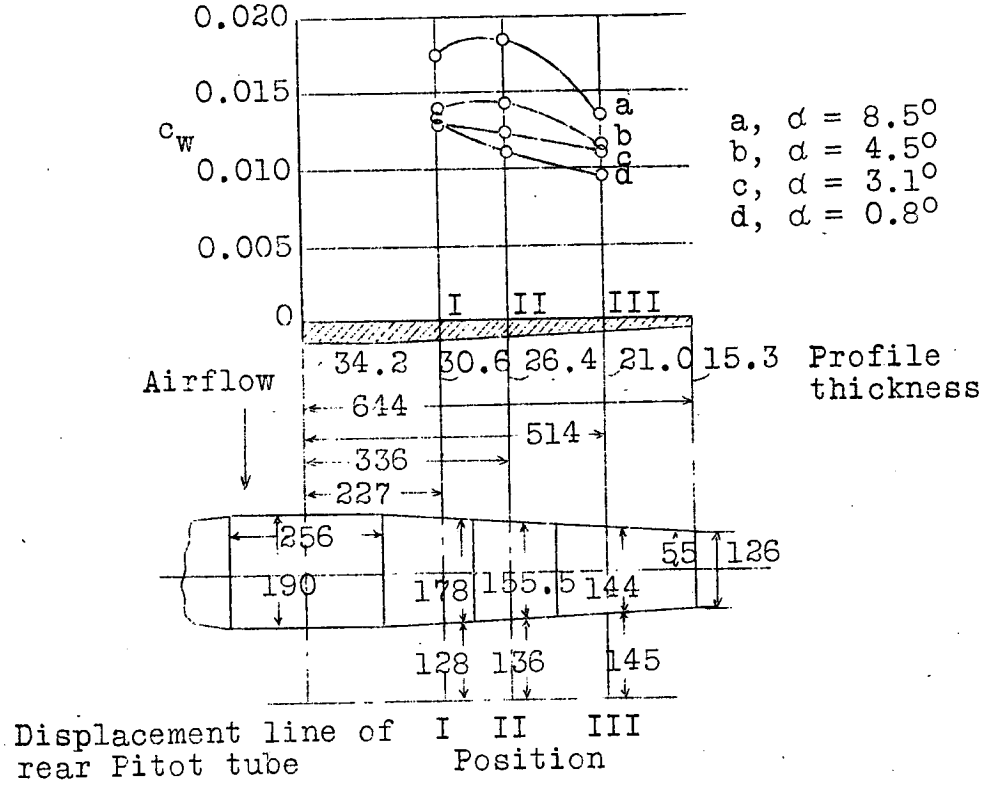

Fig.9 Distribution of the profile drag along the span.

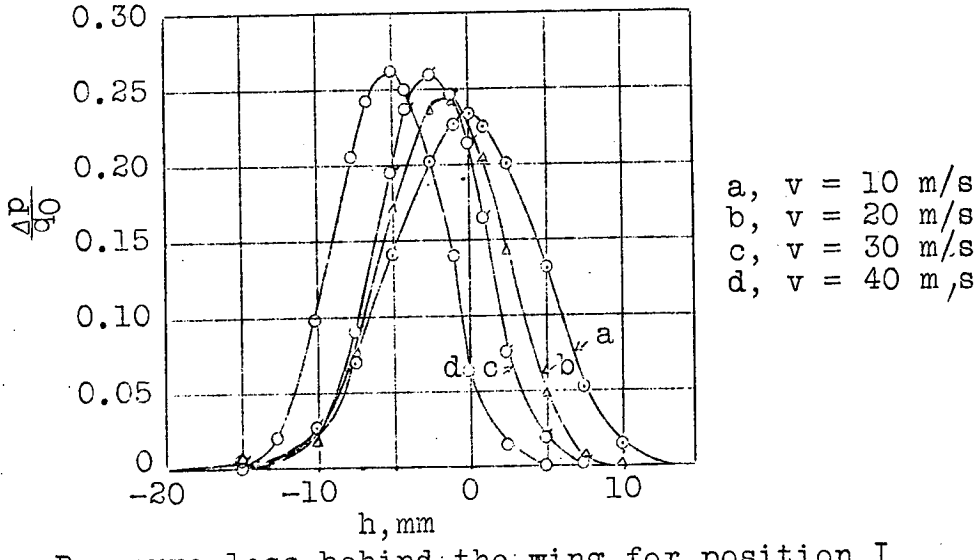

Fig.10 Pressure loss behind the wing for position I of the Pitot tubes for four different velocities and $\alpha = 0.8^{\circ}$.

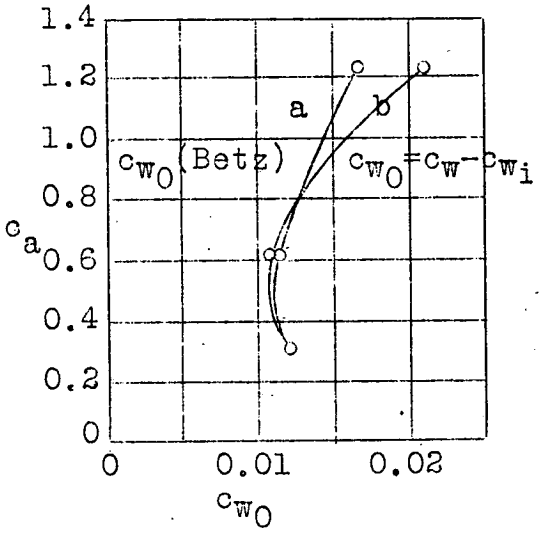

Fig.11 Comparison of results obtained by momentum measurements (a) and by full measurements (b) on a A20 wing model.

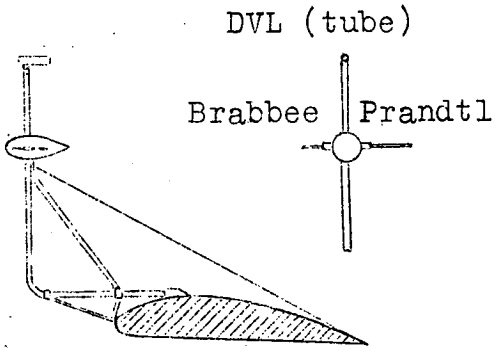

Fig.13 Arrangement of the measuring instruments (tubes) in front of the left wing of a Junkers A20.

Fig.20

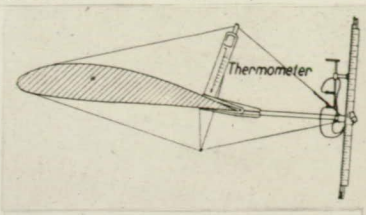

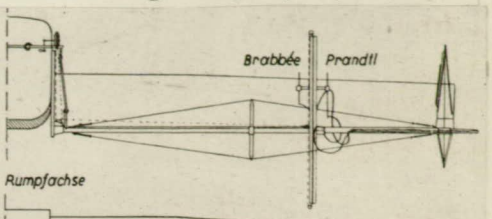

Fig.15 Installation behind right wing.

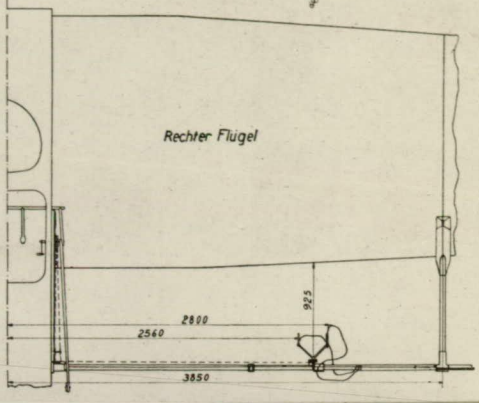

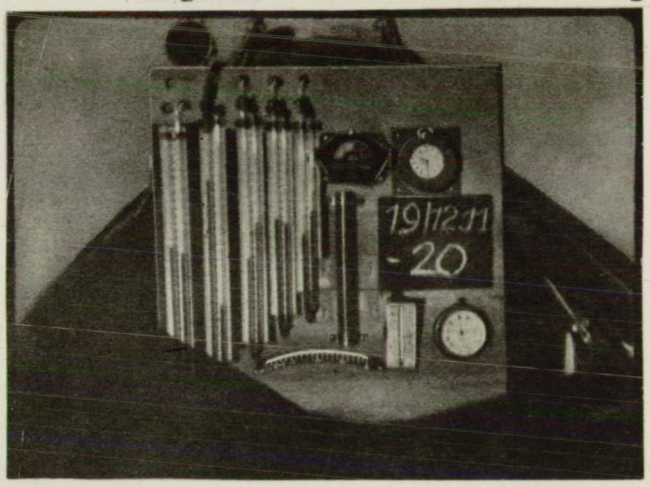

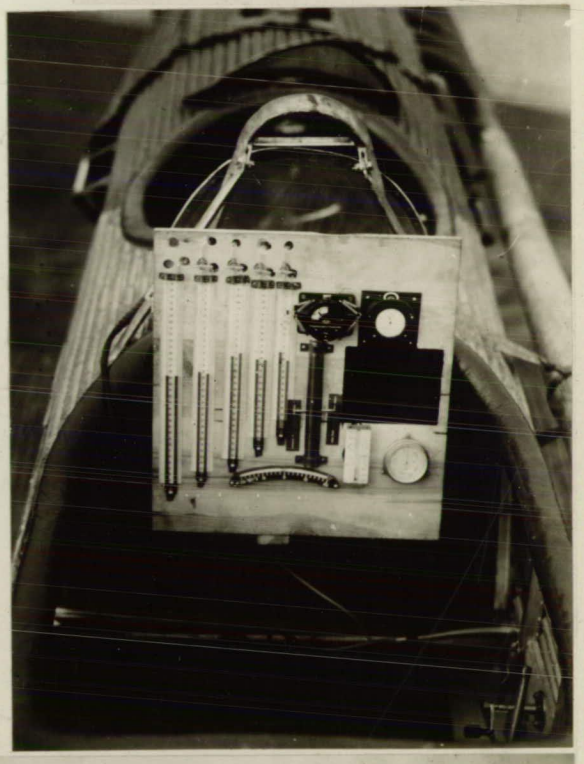

Fig.19

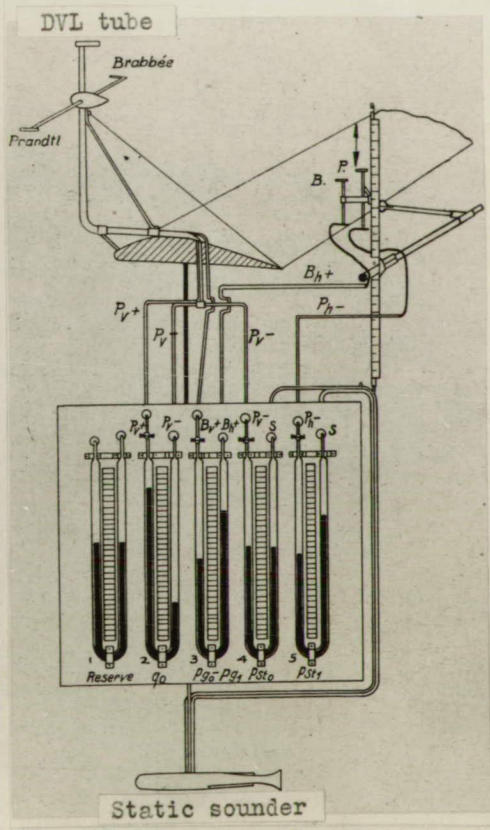

Fig.18 Diagram of manometers and piping.

Fig.23

5660 A.S.

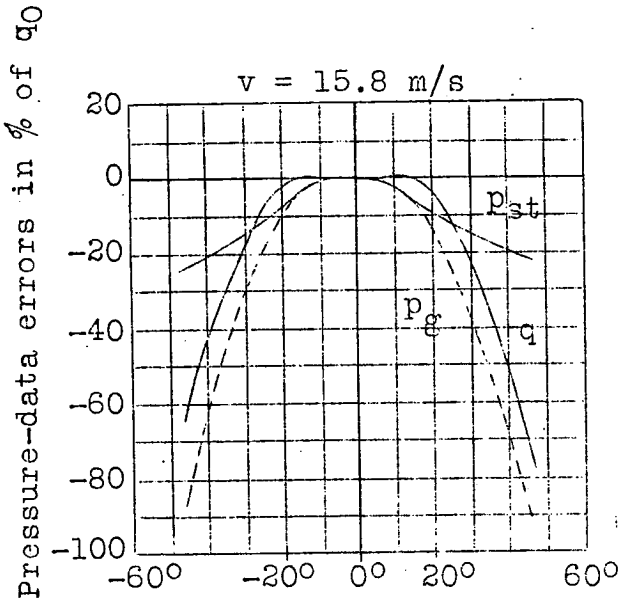

Fig.21 Prandtl pressure tube.

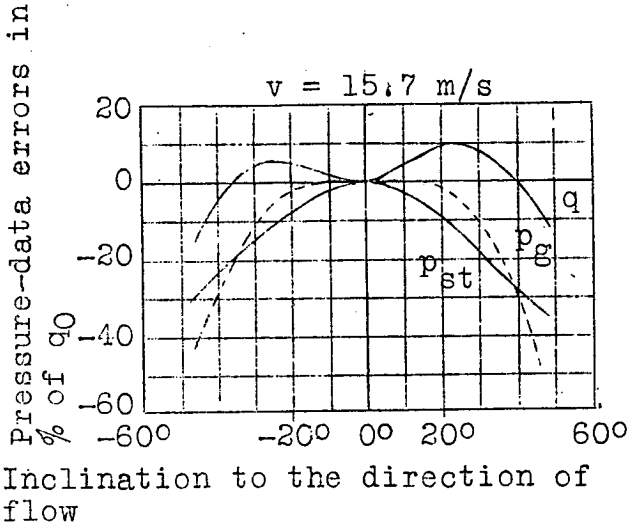

Fig.22 Brabbée pressure tube.

A, Flight 19· c_a = 0.39
B, " 12II " = 0.46
C, " 16 " = 0.42
D, " 12I " = 0.60
E, " 14 " = 0.57
F, " 17 " = 0.70

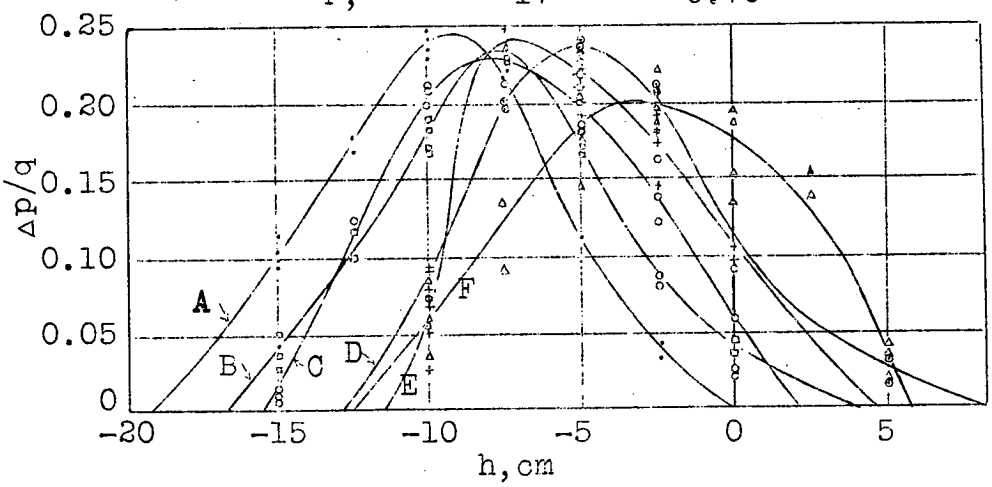

Fig.24 Comparative pressure decrease behind the wing. Result of flight test.

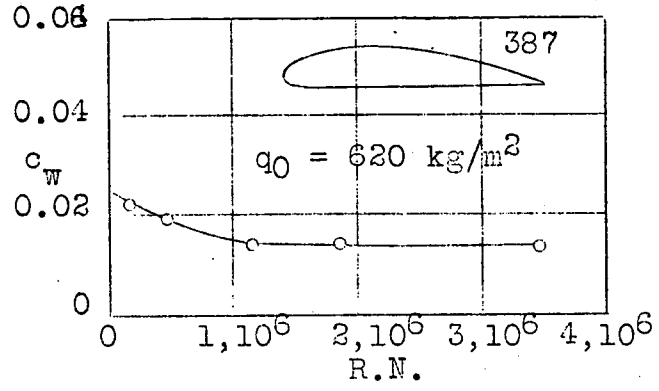

Fig.26 Test of the Göttingen section 387 in the variable-density wind tunnel at 19.8 atmos.

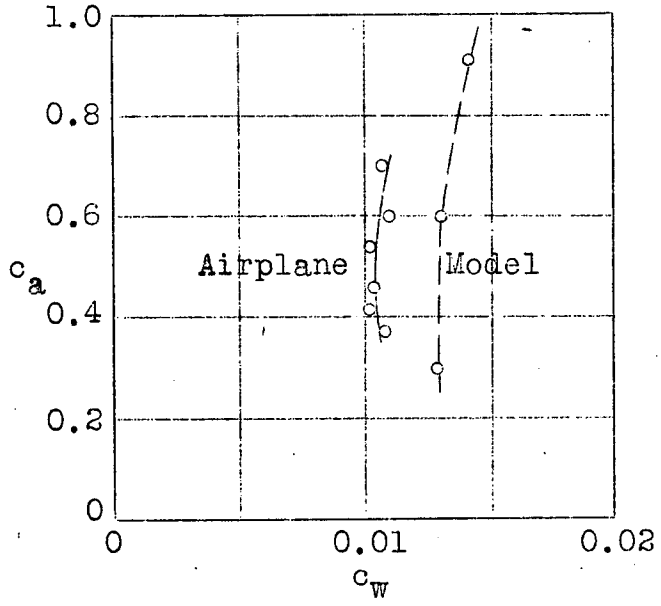

Fig.25 Comparison of measurements for position I of the pressure tubes.